Karaca et al. BMC Musculoskeletal Disorders (2026) 27:286
https://doi.org/10.1186/s12891-026-09681-5

BMC Musculoskeletal Disorders

RESEARCH

Open Access

Biomechanical comparison of different fixation methods for tibiofibular syndesmosis injuries: a finite element analysis study

Halil Karaca[1*], Cem Zeki Esenyel[2], Levent Ugur[3], Kursad Aytekin[4], Emre Kurt[5] and Tugcan Demir[4]

Abstract

Background Syndesmosis injuries require effective fixation to restore ankle stability and function. Therefore, the aim of this study was to use the finite element method to evaluate and compare the biomechanical efficiency of three different fixation techniques used to treat syndesmosis injuries: ANK nails, cortical screws, and suture buttons.

Methods A three-dimensional model of the ankle complex of a healthy individual was created from computed tomography (CT) images for finite element analysis (FEA). In the model, the tibia, fibula, talus, calcaneus, and navicular bones and ligament structures were modeled according to anatomical data. Sikka stage-4 syndesmosis injury was simulated by removing the anterior inferior tibiofibular ligament (AITFL), posterior inferior tibiofibular ligament (PITFL), transverse tibiofibular ligament (TTFL), interosseous ligament (IOL), and deltoid ligament. Eight different implant configurations were modeled for fixation, which included ANK nails, cortical screws, and suture buttons. During loading, compressive and tangential forces were applied to the tibial plateau by simulating the midstance phase of gait. Lateral and posterior fibular translation, external rotation, and the joint reaction force (JRF) were evaluated.

Results Compared with the intact model, the lateral translation and external fibular rotation were more restricted by the use of two screws, whereas posterior fibular translation was more restricted by the use of the ANK nail. The screw and ANK nails provided rigid fixation, whereas the suture button allowed flexible fixation. The rigid fixation methods resulted in a more pronounced increase in JRFs. Anatomical suture-button (ANSB) fixation achieved the closest biomechanical parameters to those of the intact ankle model.

Discussion In the treatment of syndesmosis injuries, ANSB fixation stands out as a method that balances stability with natural joint motion. While rigid fixation methods lead to high joint reaction forces, the ANSB model provides advantages in terms of long-term joint health by providing better preservation of physiological mobility.

Keywords Syndesmosis, Finite element analysis, Screw, Suture button

*Correspondence:
Halil Karaca
halilkrc52@gmail.com
[1]Department of Orthopaedics and Traumatology, Arhavi State Hospital, Artvin, Turkey
[2]Department of Orthopaedics and Traumatolog, Medical Park Ordu Hospital, Ordu, Turkey
[3]Department of Mechanical Engineering, Faculty of Engineering, Amasya University, Amasya, Turkey
[4]Department of Orthopaedics and Traumatology, Giresun University, Giresun , Turkey
[5]Department of Orthopaedics and Traumatology, Sinop State Hospital, Sinop, Turkey

Introduction

Distal tibiofibular syndesmosis plays an important role in maintaining ankle stability. Distal tibiofibular syndesmosis injuries often occur after high-energy injuries. Syndesmosis injuries may be isolated injuries and may be associated with malleolar fractures or deltoid ligament injuries [1, 2]. Such injuries account for approximately 1–18% of all ankle lesions [3, 4], and recent studies show that their incidence is in the range of 17–74% of all sports injuries of the ankle [5, 6]. Syndesmosis injuries that are not appropriately treated can lead to instability of the syndesmosis, tibiofibular diastasis, and talar shift, which have all been associated with poor functional outcomes. Therefore, appropriately treating tibiofibular syndesmosis injuries is essential [7–9].

The aim of treatment for ankle syndesmosis injuries is to restore the biomechanics of the ankle. The treatment method should prevent tibiofibular diastasis, allow for physiological fibular movement, and prevent an increase in reaction forces at the tibiotalar joint. To achieve these aims, clinical and biomechanical studies are being conducted to establish the optimal approach for surgical treatment, and various implant and fixation techniques are being developed.

Screw fixation is widely regarded as the gold standard for the surgical treatment of syndesmosis injuries because of its ability to provide rigid stabilization and maintain reduction. However, this method has several limitations, such as screw loosening, breakage, patient discomfort, tibiofibular synostosis, late diastasis, and loss of reduction [10–13]. These drawbacks have motivated continuing investigations into alternative fixation techniques that can offer comparable stability while minimizing hardware-related complications.

The suture button was developed to avoid these complications and has potential advantages of allowing physiological movement, providing adequate stability, earlier rehabilitation, and less need for implant removal [14–16]. These advantages have led to increasing use of suture buttons in the treatment of syndesmosis injuries [17]. One of the less commonly used fixation methods is the ANK nail method, which was developed for the treatment of lateral malleolar fractures associated with syndesmotic injuries. It has been reported that this method does not cause skin problems, that implant failure is not observed, and that it is economical [18, 19].

The aim of this study is to use finite element analysis (FEA) for biomechanical comparison of three different fixation methods: ANK nails, screws, and suture buttons. The findings could potentially guide clinical decision making by determining the fixation strategy that best restores ankle joint stability.

Methods

Creation of 3D reconstruction

Ethical approval was obtained from the Clinical Research Ethics Committee of Giresun University (Decision No: KAEK-51). A diagram of the methodology used in the study is shown in Fig. 1. Computed tomography (CT) images of a healthy adult male were obtained from the right sole of the foot to the level of the knee joint at cross-sectional intervals of 0.5 mm. The CT sections were scanned in the Digital Imaging and Communications in Medicine (DICOM) format with 0.75-mm pixel size at 120 kV with raw data resolution of 512 × 512 pixels. A total of 1000 sections were obtained. The sections were used in MIMICS® 12.11 (Materialise's Interactive Medical Image Control System/Materialise NV, Belgium) to create 3D models of the tibia, fibula, talus, calcaneus, and navicular region (Fig. 2).

The unwanted geometries in the 3D models of the tibia, fibula, talus, calcaneus, and navicular bones were edited to obtain the correct geometry. The editing was done by converting the geometries from MIMICS software format to the stereolithography format and sent to the reverse engineering software GEOMAGIC® Studio. NURBS (nonuniform rational B-spline) surfaces were obtained by completing processes such as filling gaps, removing sharpness, correcting the roughness of the surfaces, and revising surface overlaps using the reverse

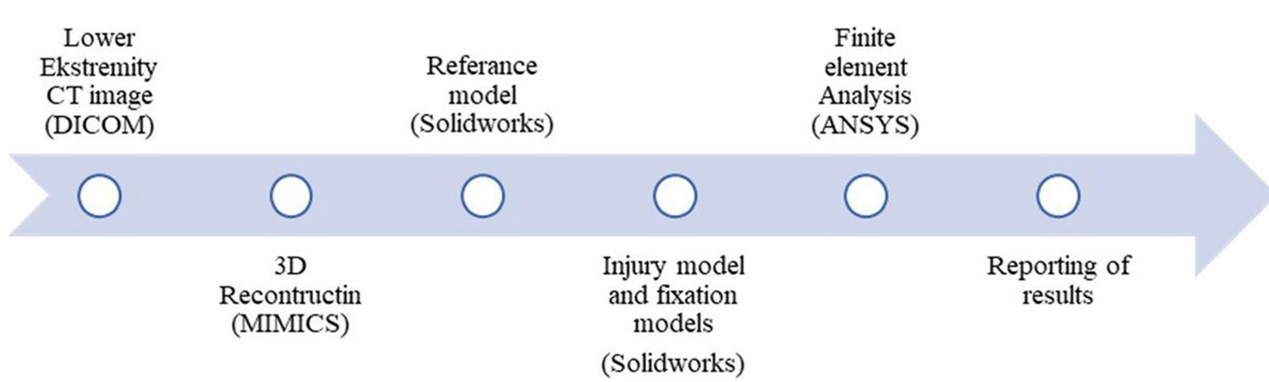

Fig. 1 Flow chart of materials and methods

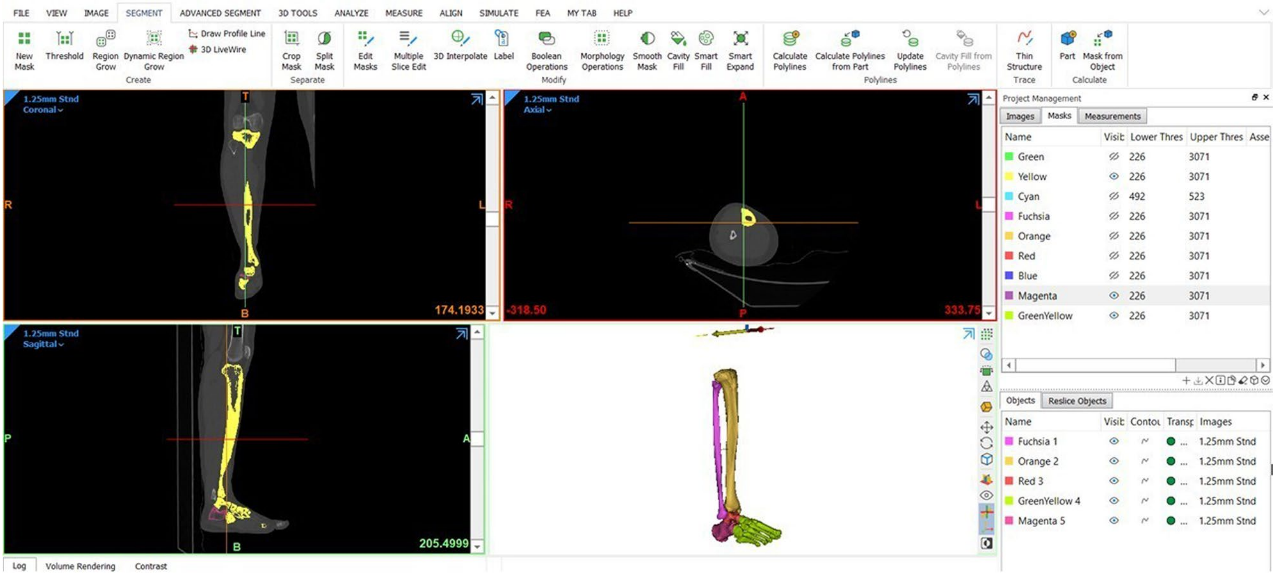

Fig. 2 Reconstruction of bone model from CT scan

Table 1 Material properties of ligaments

Ligament	Young's Modulus (E) MPa	Poisson's ratio (v)
Anterior inferior tibiofibular	160	0.49
Posterior inferior tibiofibular	160	0.49
Interosseous	260	0.4
Anterior talofibular	255.5	0.49
Posterior talofibular	216.5	0.49
Calcaneofibular	512	0.49
Interosseous talocalcaneal	260	0.4
Lateral talocalcaneal	260	0.4
Posterior talocalcaneal	260	0.4
Medial talocalcaneal	260	0.4
Talonavicular ligament	260	0.4
Anterior tibiotalar	184.5	0.49
Posterior tibiotalar	99.5	0.49
Tibiocalcaneal	512	0.49
Calcaneonavicular	260	0.4
Interosseous membrane	260	0.4
Transvers tibiofibular	160	0.49
Cervical	260	0.4

engineering software. The bone models were sent to SolidWorks® software (Dassault Systems, USA) to create a 3D bone model of the ankle.

Creation of the reference model

The attachment sites of the ligaments on the bones were determined according to anatomical atlas drawings and dissection studies [20–24]. Ligaments were designed as a 3D solid model in SolidWorks in accordance with the anatomical structure. The mechanical properties of the ligaments were defined based on values from the literature (Table 1) [25–30].

Creation of the mesh structure and material properties

A mesh structure was created for the obtained ankle model using ANSYS Workbench (Version 19, Ansys Inc., USA) for FEA. To assess mesh sensitivity, element sizes were varied in 0.25 mm increments. Initial element sizes were selected as 3 mm for bone structures and 1.5 mm for implants (screws and buttons). The mesh convergence study was based on changes joint reaction force values. As shown in Fig. 3, convergence was achieved when the mesh contained approximately 677,386 tetrahedral elements and 1,082,100 nodes, corresponding to an optimal element size of 1.5 mm for bone and 0.75 mm for implants (Fig. 4).

High-order 10-node Solid187 tetrahedral elements were used to ensure simulation accuracy, and the average mesh quality was 0.81, indicating sufficient refinement. All simulations were conducted under nonlinear static loading using the Newton–Raphson method. Material properties were defined as isotropic, homogeneous, and linearly elastic, based on values from the literature (Table 2). The final mesh configuration aligns with validated finite element studies reported in previous research [31–34], supporting the reliability and reproducibility of the current model.

Injury model

The aim of the study was to compare treatment methods in conditions of severe instability. Sikka Grade 4 syndesmotic injury was simulated by removing the AITFL, PITFL, TTFL, IOL, and deltoid ligament from the injury

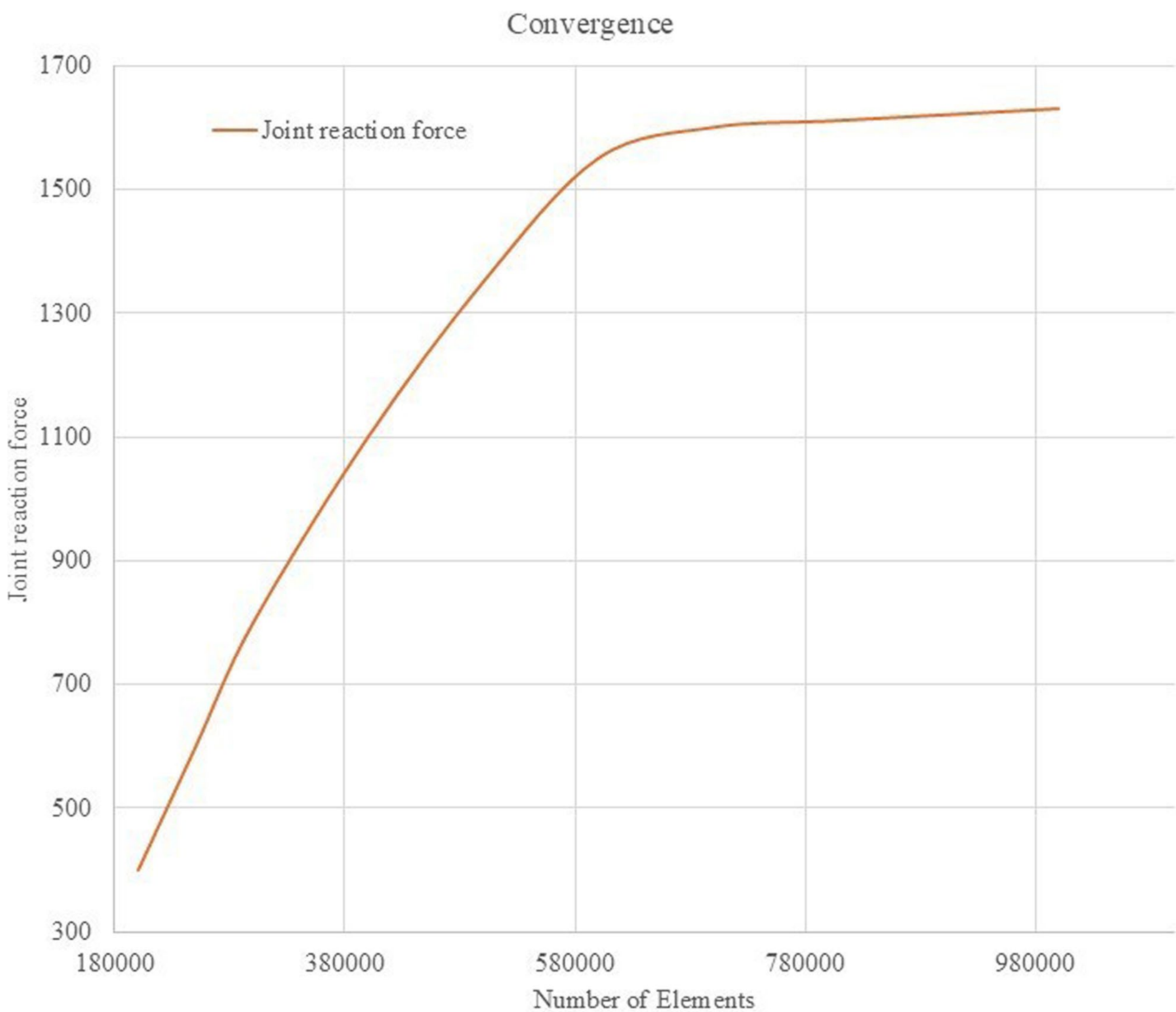

Fig. 3 Convergence study results in FEA

Fig. 4 Mesh structure model; the reference model contained 677,386 tetrahedral elements and 1,082,100 nodes

Table 2 Properties of implant materials

Material	Young's Modulus (E) MPa	Poisson's ratio (v)
Cortical bone	17,000	0.3
Cancellous bone	700	0.2
No. 5 FiberWire	380,000	0,39
Suture-button titanium	96,000	0.36
Titanium	106,000	0.33

model [35]. Although screw fixation is frequently preferred in the surgical treatment of syndesmosis injuries, the frequency of suture-button use has been increasing in recent years. However, the optimal number and level of screws and the number and orientation of suture buttons are debated. Therefore, models were created using different numbers and levels of screws and different numbers and orientations of the suture button.

Model validation

To evaluate the reliability of the developed FE model, a multi-stage validation strategy was implemented, involving numerical validation, mesh convergence analysis, and comparison with published experimental and computational data obtained under similar loading conditions. Four primary biomechanical variables, lateral fibular translation (LFT), posterior fibular translation (PFT), external rotation (ER), and joint reaction force (JRF), were compared with values reported in the literature.

Relatively few studies have evaluated syndesmotic injury during the mid-stance phase under loading conditions comparable to those applied in the present investigation [36, 37]. Given the methodological similarity in loading configuration, injury simulation, and evaluated parameters between our study and that of Mercan et al. [37], comparison with their findings provides an appropriate reference for kinematic validation.

In the current model, LFT increased from 0.62 mm to 1.02 mm (64.5%), whereas Mercan et al. reported an increase from 0.54 mm to 0.91 mm (68.5%). Similarly, PFT increased from 0.29 mm to 0.47 mm (62.1%) in our model, while their study demonstrated an increase from 0.43 mm to 0.64 mm (48.8%) [37]. Additionally, the cadaveric biomechanical study by Ebramzadeh et al. reported that tibiofibular diastasis remained below 1.0 mm in the intact state and below 2.0 mm under cyclic loading across all fixation groups, indicating limited separation under controlled loading conditions [38]. Together, the comparable percentage changes in the finite element analysis and the agreement with cadaveric translational values indicate the biomechanical consistency and physiological validity of our model.

Cadaver studies indicate that syndesmotic instability should be evaluated as a multi-planar structure involving lateral and posterior translation and rotation [1]. In our injured and intact model, the increase in LFT, PFT, and ER reproduces this multidimensional instability pattern and demonstrates biomechanical consistency with previously reported experimental findings.

External rotation is highly dependent on the loading configuration; values of 1.59 ± 0.67° have been reported under isolated axial compression, whereas rotation increases to approximately 4.7° when controlled external torque is applied [39, 40]. In our study, the injured model demonstrated an ER of 2.41°, which yansıtmaktadır an appropriate intermediate response between compression and torque-dependent conditions.

To simulate the mid-stance load, a compression load of 2352 N was applied, which resulted in a joint reaction force of 1550 N (approximately 66% of the applied load) in the intact model. This finding is consistent with previously reported computational and gait-based studies showing that mid-stance ankle joint reaction forces range between 60 and 80% of body weight [41, 42]. After syndesmotic injury, alterations in the magnitude of joint reaction force are observed, consistent with experimental findings demonstrating disrupted tibiotalar load transmission and its restoration following fixation [43].

In conclusion, the concordance in translational behavior, the biomechanically consistent rotational response, and the physiologically consistent joint reaction force pattern collectively confirm the biomechanical robustness and physiological credibility of the developed FE model.

Fixation models

The proper screw position is traditionally described as 2–4 cm proximal and parallel to the tibial plafond, angled 20–30° anteromedially along the trans-malleolar axis [44, 45]. Most surgeons insert 1 or 2 screws 2.1–4.0 cm proximal to the tibial plafond [46]. In recent years, 3.5-mm screws have been preferred more frequently [47].

In the present study, 3.5-mm screws were placed 2–4 cm proximal to the tibial plafond parallel to the tibiotalar joint in the coronal plane with a 30° anteromedial orientation in the transverse plane. To compare the biomechanical effects of the implants individually and in combination, screws and suture buttons were applied at the same distance from the tibial plafond. Eight fixation models were created (Table 3; Fig. 5).

ANK nail application was performed as follows; A nail entry point was created 5 mm proximal to the tip of the lateral malleolus, and a 2.5-mm Kirschner wire was introduced through this entry and advanced intramedullary into the fibular canal. Subsequentl, a 3.5-mm bicortical screw (with its length confirmed using a depth gauge) was inserted, and the ANK nail was secured to the anterolateral surface of the distal tibia [18]. The screw

Table 3 Anatomical levels and orientations of fixation models

Model	level	Orientation
Distal screw (DS)	2 cm	30° anteromedial
Proksimal screw (PS)	4 cm	30° anteromedial
Double screw (PSDS)	2 and 4 cm	30° anteromedial
Suture button (SB)	2 cm	30° anteromedial
Parallel suture button (PLSB)	2 and 4 cm	30° anteromedial
Divergent suture button (DJSB)	2 and 4 cm	distal 30° anteromedial proksimal 45° anteromedial
Anatomical suture button (ANSB)	anatomical	Anatomical
ANK nail (ANK-N)	N/A	N/A

cm centimeter

was inserted 5 mm superomedial to the anterolateral capsular ridge of the distal tibia.

Several biomechanical studies have investigated how the number and orientation of suture buttons affect syndesmotic stability [37, 47–51]. In the single suture-button model, the implant was positioned 2 cm proximal to the tibial plafond. In the parallel suture-button configuration, two implants were placed 2 cm and 4 cm proximal to the plafond, respectively, and were oriented parallel to the tibiotalar joint in the coronal plane with a 30° anteromedial trajectory in the transverse plane [51]. Teramoto et al. described a divergent suture-button configuration, in which a suture-button was placed 2 cm proximal to the tibial plafond with a 30° anteromedial orientation, followed by a second suture-button positioned more proximally with a 45° anteromedial orientation [48]. The suture button, parallel suture button, and divergent suture button models included in our study were created based on these studies.

In science and medicine, a normal physiological state is often mimicked to achieve maximum efficiency. We used this idea for the treatment of ankle syndesmosis injuries as a basis to create an anatomical suture-button (ANSB) model. Williams et al. anatomically defined the attachment sites of the AITFL and PITFL in the tibia and fibula [23]. Teramoto et al. described the suture button

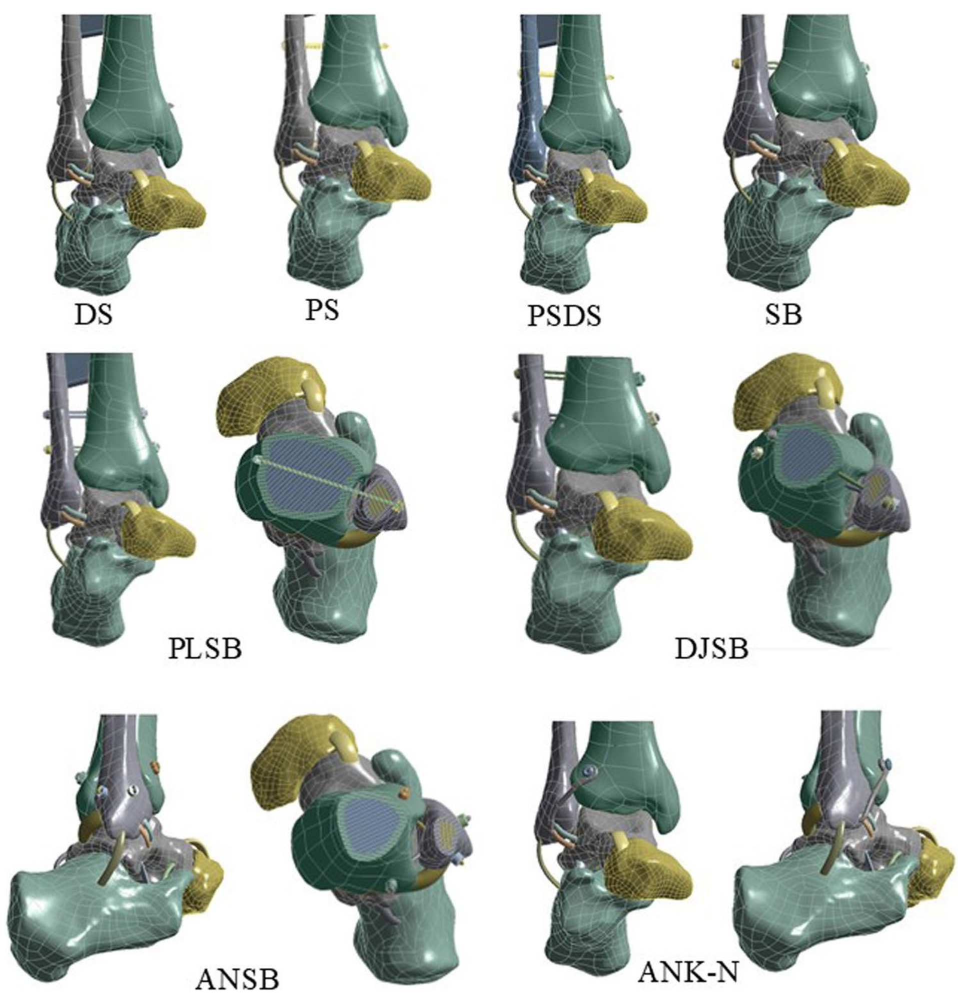

Fig. 5 Fixation models. DS; Distal screw, PS; Proksimal screw, PSDS; Double screw, SB; Suture button, PLSB; Parallel suture button, DJSB; Divergent suture button, ANSB; Anatomical suture button, ANK-N; ANK nail

as extending between the posterolateral aspect of the fibula and the anterolateral aspect of the tibia in an anatomical suture-button model mimicking the AITFL [48]. Furthermore, Kikuchi et al. defined the tibial and fibular attachment sites of the AITFL and PITFL identified the insertion centers of these ligaments on the bone [52]. While these defined points denote the centers of the ligament insertion sites, it should be noted that the tibial attachment of these ligaments spans a wider anatomical area [53, 54]. On the tibial side, the anterior capsular ridge and the Chaput's and Volkmann's tubercles were reported as distinct and reliable osseous landmarks for the insertion sites of the AITFL and PITFL [52]. These bony prominences serve as important anatomical reference points during surgery, facilitating implant placement and guiding the surgical procedures. In our study, when determining the implantation points for the suture buttons, we considered both the ligament insertion sites defined in the literature and the aforementioned osseous landmarks.

Taking all these anatomical considerations into account, the ANSB model was constructed as follows: The implantation points on the tibia and fibula were selected to replicate the anatomical orientation of the AITFL and PITFL. For the AITFL, the fibular insertion point was located 30 mm posterosuperior to the tip of the lateral malleolus, and the tibial point was placed 5 mm superomedial to the Chaput tubercle. For the PITFL, the fibular insertion point was located 26 mm anterosuperior to the tip of the lateral malleolus, and the tibial point was located 5 mm superomedial to the Volkmann tubercle.

Creation of finite element models

The finite element models were developed using data from the midstance phase, which is the third phase of the stance phase of walking. With the ankle in a neutral position, a compressive force of 2352 Newtons (N) and a tangential force of 235 N were applied to the tibial plateau [55]. To apply the knee load physiologically, 60% of the compressive force was distributed to the medial plateau of the tibia, and 40% was distributed to the lateral plateau of the tibia [56]. All bones moved around the calcaneus and were constrained at the plantar surface, while the navicular bones were constrained at the anterior surface (Fig. 6). The internal–external rotation of the tibia was also constrained.

Reporting of results

An anatomical coordinate system was defined to correctly interpret the vector changes that occur with loading. Accordingly, the x-axis was defined as parallel to the longitudinal anatomical axis of the tibia, the y-axis was defined as parallel to the longitudinal anatomical axis of the calcaneus, and the z-axis was defined as parallel to the imaginary line connecting the lateral and medial malleolar tips. Translation and rotation were measured on axial CT images obtained 1 cm proximal to the tibial plafond, using a standardized anatomical coordinate system

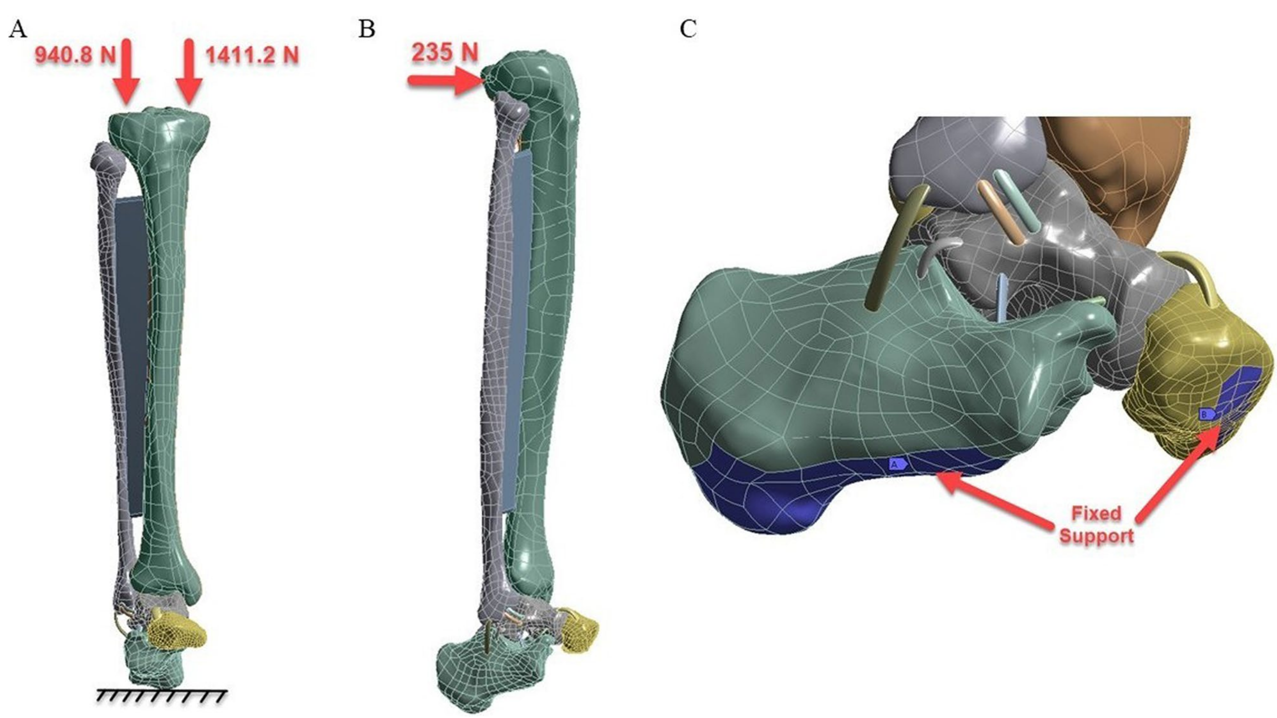

Fig. 6 Loading and boundary conditions of the model. Compressive force of 2352 N (**A**) and tangential force of 235 N (**B**) were applied to the tibial plateau. Calcaneus restricted from the plantar surface and the navicular restricted from the anterior surface (**C**)

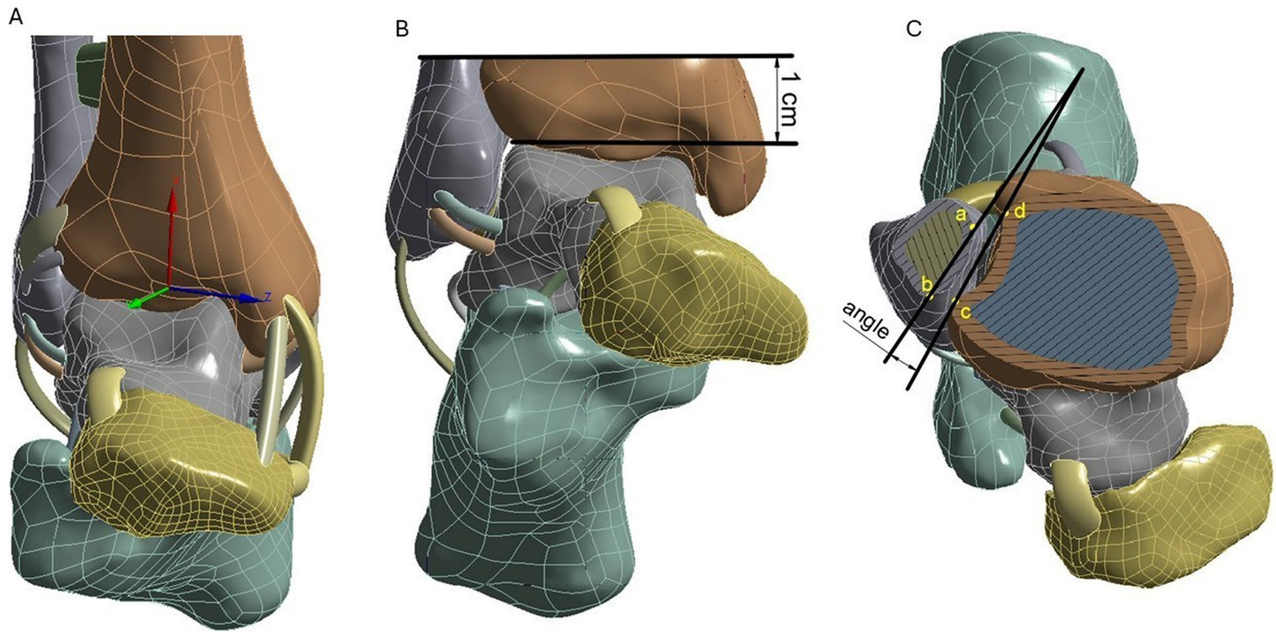

Fig. 7 Defining of the anatomical coordinate system (**A**), measurements 1 cm proximal to the tibial plafond (**B**), angular measurement method of rotational changes in the tibia and fibula after loading. c, most anterior point of the incisura, b, most anterior point of the fibula closest to c, d, most posterior point of the incisura, a, most posterior point of the fibula closest to d angle; the angle between imaginary lines connecting points defined on the tibia and fibula (**C**) fibular rotation angle; difference between before and after loading angles

established for the tibia and fibula. The lateral fibular translation (LFT) and posterior fibular translation (PFT) values were considered as the relative values obtained by subtracting the tibia displacement values from the displacement values in the fibula if their movements are in the same direction and by summing the displacement values in the fibula with the tibia displacement values if the movements are in the opposite direction. The external fibular rotation (EFR) values were obtained according to the methodology defined by Nault et al. [57]. To quantify rotational changes following loading, four anatomical landmarks were identified on the axial section: point c was defined as the most anterior point of the tibial incisura, point b as the most anterior point of the fibula closest to point c, point d as the most posterior point of the tibial incisura, and point a as the most posterior point of the fibula closest to point d. Using these landmarks, two imaginary reference lines were drawn: one connecting a–b and the other connecting c–d. The angle formed between these two lines represented the rotational alignment at the level of the syndesmosis (Fig. 7). For each model, this angle was measured both before loading and after loading. The fibular rotation angle was then calculated by subtracting the pre-loading value from the post-loading value.

Table 4 Translations, rotations, and joint reaction forces in the intact, injured, and treated models

model	Lateral fibular translation (mm)	Posterior fibular translation (mm)	External fibular rotation (°)	Joint Reaction Force (*N*)
Intact	0,62	0,29	0,47	1550
Injured	1,02	0,47	2,41	2396
DS	0,42	0,15	0,16	2123
PS	0,52	0,20	0,30	2037
PSDS	0,33	0,13	0,15	2204
SB	0,69	0,35	0,60	1824
PLSB	0,70	0,40	0,52	1715
DJSB	0,69	0,39	0,61	1938
ANSB	0,57	0,26	0,49	1675
ANK-N	0,44	0,12	0,28	2084

mm millimeter, *N* Newton

Results

Lateral fibular translation (LFT)

Table 4 shows the values of LFT, PFT, EFR, and JRF that occur in the fibula when forces acting on the tibial plateau during the mid-stance phase are applied. Greater LFTs were observed in the injured model than in the intact model. Among the screw models, the values closest to those of the intact model (0.62 mm) were obtained in the PS model (0.52 mm). The model with the most restrictions was the PSDS model with 2 screws (0.33 mm).

The ANK nail (0.44 mm) provided a similar restriction to the distal screw (0.42 mm) applied at 2 cm. Greater

LFTs occurred in the suture button models than in the screw and ANK nail models. Among all the treatment methods, the values closest to those of the intact model (0.62 mm) were obtained in the ANSB model (0.57 mm). Similar values were obtained for the PLSB (0.70 mm) and DJSB (0.69 mm) models, where two suture buttons were applied at 2 and 4 cm, or one suture button (0.69 mm) was applied at 2 cm.

Posterior fibular translation (PFT)

Compared with the solid model (0.29 mm), less PFT was observed in the screw model. Among the screw models, the PSDS model (0.13 mm) restricted PFT the most. The distal screw (0.15 mm) restricted PFT more than the proximal screw (0.20 mm). In the suture button models, greater PFTs were observed than in the solid model. In the PLSB (0.40) and DJSB (0.39) models with two suture buttons, greater PFT was observed than in the model with one suture button (0.35 mm). The greatest restriction in PFT was observed in the ANK-N model (0.12 mm). Among all the treatment methods, the values closest to those of the intact model (0.29 mm) were obtained with the ANSB model (0.26 mm).

External fibular rotation (EFR)

EFR increased after injury and decreased with the application of the treatments. In the suture-button models, more EFR occurred than in the ANK nail and screw models. The treatment method that restricted the EFR the most was the PSDS model. Among all the treatment methods, the values closest to those of the intact model (0.47°) were obtained with the ANSB model (0.49°). The ANK nail and screw restricted the EFR more than the intact model did.

Joint reaction force (JRF)

An increase in JRF was observed in the injured model (2396 N) compared with the intact model (1550 N). All treatments reduced the increase in JRF after injury. Higher JRF values were obtained in the ANK-nail and screw models than in the suture-button models. The highest JRF value among the treatment models was obtained with the PSDS model (2204 N). The values closest to those of the intact model were observed in the ANSB model (1675 N). Higher JRF values were observed in models with lower LFT and PFT values.

Correlation analyses were performed to assess the relationship between fibular translations and JRF. No significant correlation was observed between LFT and JRF (Spearman's ρ = -0.27, $p = 0.46$) or between PFT and JRF (Spearman's ρ = -0.22, $p = 0.53$).

Discussion

Among the surgical treatment options used for syndesmosis injuries, values close to those of a stable ankle joint were obtained via ANSB fixation in terms of translation and JRFs. The effectiveness of the ANK nail was compared with those of other treatment methods for the first time, and it was observed to provide rigid fixation similar to screws. Our study makes an important contribution to the literature by comparing the effects of different fixation methods on JRFs. Greater JRFs were observed with screws and ANK nails, which have greater restriction compared to suture buttons.

Consistent with the literature, ankle syndesmosis injury caused increased movement of the fibula. After fixation with screws, movement in the medial/lateral and anterior/posterior directions and external rotation decreased [58]. Consistent with the results of McBryde et al. placing the screw close to the joint resulted in more rigid fixation during syndesmosis [59]. When three different screw configurations were examined, lateral translation, posterior translation, and external rotation values closest to those of the intact model were observed in the 4-cm screw model, which is consistent with the findings of Mercan et al. [37]. More physiological values were obtained with a 4-cm screw, which should be considered when planning screw fixation for the treatment of syndesmotic injuries.

It has been reported that the use of two screws in syndesmotic injuries results in less syndesmotic widening compared to the use of one screw [36, 37, 60]. Similarly, in the present study, the use of two screws caused greater restriction in the syndesmosis compared to other treatment methods. Although biomechanical studies have shown that two screws provide greater stability in the syndesmotic joint, increasing the number of screws does not improve functional outcomes [61, 62]. Similarly, in the present study, the most rigid fixation was achieved with two screws. In addition, the increase in JRF was greater than that observed with the other treatment methods. Therefore, the use of double screws may be limited to patients who are at high risk of screw failure, such as obese patients.

Whether syndesmotic screws should be removed or retained remains controversial. While Wójtowicz et al. reported no functional benefit following screw removal [63], Sanda et al. associated removal with improved mobility, better performance of daily activities, and reduced postoperative pain and anxiety [64]. Additionally, higher rates of osteolysis have been reported in patients in whom screws were retained [65, 66].

In the present study, increased restriction of syndesmotic motion was associated with higher JRFs, with screw fixation demonstrating a greater increase in JRF compared to suture-button fixation. These findings suggest that decisions regarding screw removal should be individualized, taking patient-specific clinical and biomechanical factors into consideration rather than applying a uniform management strategy.

A study evaluating the number and configuration of suture buttons compared three different suture-button fixation techniques (single suture button, parallel double suture buttons, and diverging double suture buttons) and found no significant difference in stability among the treatment methods [49]. Another study reported that increasing the number of suture buttons was associated with improved stability and emphasized that the orientation of the suture buttons plays an important role in achieving stability [36]. Mercan et al. reported that in double suture-button fixation applied with a parallel configuration, the proximally placed suture button did not contribute to syndesmotic fixation [37]. In the present study, the application of a second suture button resulted in similar lateral translation values, while an increase in posterior translation was observed. Our results suggest that the addition of a second proximally applied suture button does not confer a meaningful additional contribution to syndesmotic stability.

Finite element and biomechanical studies comparing suture-button and screw fixation for syndesmosis stabilization have reported that screw fixation results in less syndesmotic widening compared with suture-button fixation, a finding that is consistent with the biomechanical results of the present study [67–70]. Nevertheless, it should be acknowledged that data derived from biomechanical analyses may not directly translate into functional or clinical outcomes. Indeed, several clinical studies have reported that syndesmotic fixation performed with either suture-button or screw techniques results in comparable clinical outcomes [71, 72].

The ANK nail was developed for the treatment of lateral malleolar fractures with syndesmotic injuries and has been associated with good functional outcomes [18, 19]. The present study is the first to evaluate the efficacy of ANK nails in comparison to other treatment methods. Less translation and external rotation were observed in the ANK-nail fixation model than in the intact model, similar to screw fixation, and this treatment method had the least posterior translation.

The ANK nail represents an extra-articular fixation strategy and is conceptually distinct from trans-syndesmotic techniques. Nevertheless, extra-articular stabilization approaches have been investigated in the literature as biomechanically relevant alternatives to trans-syndesmotic fixation. In a biomechanical study comparing syndesmotic staple fixation, an extra-articular method, with trans-syndesmotic screw fixation, staple application was reported to provide sufficient syndesmotic stability [73]. Furthermore, extra-articular fixation methods have been associated with lower rates of heterotopic ossification, tibiofibular synostosis, and chronic pain in the syndesmotic region [74]. However, extra-articular fixation cannot be assumed to fully reproduce the biomechanical characteristics of intra-syndesmotic constructs, and the findings should be interpreted within this conceptual limitation.

Although this was not a direct finding of the present study, considering that the ANK nail exhibits biomechanical properties that can maintain alignment in the fibula and provide stability in the syndesmosis, it can be considered an important option in the treatment of Maisonneuve fractures involving the middle third fibular shaft. In such fractures, open reduction and internal fixation are often preferred. However, more soft tissue and peroneal nerve dissection are needed for anatomical reduction of the fibula in this region. A study performed for this purpose reported that syndesmosis fixation alone was sufficient even in such fractures accompanied by syndesmosis injuries [75]. The ANK nail provides fibula and syndesmosis fixation while preventing extensive dissection and possible complications at the fracture site.

In a biomechanical study, Kelly et al. reported that alterations in tibiotalar JRFs following syndesmotic injury may be restored with screw fixation [43]. In the present study, the ANSB model demonstrated JRF values closest to those of a stable ankle, whereas more rigid fixation methods, including screws and ANK nails, were associated with higher JRFs. These findings provide a comparative biomechanical perspective on how different fixation strategies influence JRFs.

Syndesmotic injuries are frequently accompanied by additional pathologies, such as osteochondral lesions of the talar dome or tibial plafond, which have been reported at relatively high rates in the literature [76–78]. Although increased JRFs observed with rigid fixation may raise theoretical concerns regarding load transmission in the presence of such concomitant injuries, finite element analyses alone cannot establish a direct relationship between altered JRFs and cartilage degeneration or clinical outcomes. Therefore, these observations should be interpreted as hypothesis-generating, highlighting the potential relevance of considering associated pathologies when selecting a fixation method, rather than implying definitive clinical consequences.

The method used to treat syndesmotic injuries should be neither too rigid nor too flexible. The approach should prevent fibular translation and rotation without being too restrictive. The main goal of treatment should be to restore balance, movements equivalent to physiological movement, and prevent an increase in JRF.

It is known that among the ligaments around the ankle, the medial ligaments play a more important role in stabilizing the ankle joint compared to the lateral ligaments

[55]. Each ligament contributing to ankle stability has a specific and distinct role within joint biomechanics. Injury to these ligaments, either isolated or in various combinations, can lead to biomechanical changes of varying magnitude and direction in the ankle joint [79].

Additionally, in different positions of the ankle joint, the bone contact surface areas and the contributions of the ligaments to joint stability show differences. The largest contact area in the ankle joint occurs during dorsiflexion [55]. Differences in the contact areas formed in different positions of the ankle joint can cause differences in translation values, primarily in joint reaction force.

Due to the complex nature of ankle kinematics during the gait cycle, simplified biomechanical models are frequently used in the literature to evaluate this process [36, 37, 55]. In this regard, the findings of our study should be interpreted with methodological limitations in mind. The effectiveness of treatment methods was evaluated using finite element analysis based on CT data from a single patient, with the ankle in a neutral position, in a model representing advanced instability. Therefore, the results obtained should not be directly generalized to different levels of instability, dynamic loading conditions, and inter-individual anatomical variations. The results of this study should only be interpreted in the context of the conditions evaluated in the study.

Furthermore, human connective tissues exhibit anisotropic and heterogeneous mechanical response. However, in the present study, ligaments were modeled as isotropic and homogeneous. The anisotropic and heterogeneous characterization of ligaments is of critical importance, particularly in studies evaluating ligament performance, risk of injury or rupture, regions of maximum stress, and the contribution of each ligament to stability. It has been reported that isotropic modeling may underestimate stresses along the fiber direction and overestimate stresses perpendicular to the fibers [80, 81]. However, in the current study, ligament structures around the ankle were not included in the injury and treatment models. In this context, the effects of ligaments on translational movements and joint reaction forces are considered to be limited and minimal within the scope of the current modeling approach. In this regard, we believe that isotropic and homogeneous modeling is meaningful and valuable in terms of comparative biomechanical results.

Moreover, fixation models applied in a computer environment may not fully reflect the technical challenges and variability of real surgical applications. The applicability of ANSB method should be tested through cadaver studies.

The correlation analysis between fibular translation and joint reaction force represents an exploratory assessment based on a single finite element model. As such, the statistical weight and external validity of these findings are limited, and the results should be interpreted cautiously rather than as confirmatory evidence.

Consequently, the present findings should be regarded as hypothesis-generating biomechanical observations and require validation through cadaveric, experimental, or multi-subject imaging-based studies.

Conclusion

In distal tibiofibular syndesmosis injuries, the appropriate fixation method is critical for restoring ankle stability and preventing long-term complications. In this study, FEA was used to compare the biomechanical performance of different fixation methods. According to the findings, the screw and ANK-nail models provided rigid fixation and were the methods that most limited fibular translation and rotation, but this rigid fixation was associated with high JRF. In contrast, the ANSB model offered a balanced solution in terms of both providing stability and preserving physiological mobility. When a fixation method for the surgical treatment of syndesmosis injuries is selected, the patient's specific anatomical and clinical conditions should be taken into account, and a balance between stability and physiological movement should be maintained. The current results suggest that ANSB application may represent a promising alternative in clinical decision-making; however, further multi-subject and experimental validation is necessary before definitive conclusions can be drawn.

Acknowledgements

None reported.

Declaration of conflicting interest

This manuscript is derived from the first author's specialization thesis in the Department of Orthopedics and Traumatology, Faculty of Medicine, Giresun University. The thesis was completed in 2024 Giresun and is available in the university's library archive. The present article represents an original publication that has not been submitted or published elsewhere in any form, and it encapsulates the core findings of the aforementioned thesis. The authors declared no potential conflicts of interest with respect to the research, authorship, and/or publication of this article. Disclosure forms for all authors are available online.

Authors' contributions

Conceptualization, H.K.,C.Z.E., and L.U.; methodology, H.K., C.Z.E., and K.A; software, L.U.; validation, H.K., T.D., and L.U.; formal analysis, H.K. and L.U.;investigation, H.K., E.K., L.U. and T.D.; resources, H.K., C.Z.E and K.A.; data curation, H.K., E.K., and L.U.; writing—original draft preparation, H.K., and T.D.;writing—review and editing, H.K., T.D., E.K.and K.A.; visualization, H.K., E.K., andL.U.; supervision, C.Z.E and T.D; project administration, H.K. and C.Z.E All authorshave read and agreed to the published version of the manuscript.

Funding

This research was supported by Giresun University Scientific Research Projects Coordination under project number SAĞ-BAP-C-230123-04.

Data availability

The data that support the findings of this study are available from the corresponding author upon reasonable request.

Declarations

Ethics approval and consent to participate
This study was approved by the Medical Research Ethics Committee of Giresun University. The research was conducted in full compliance with the ethical principles of the Declaration of Helsinki. Written informed consent was obtained from the patient for the use of CT images and participation in the study.

Consent for publication
Not applicable.

Competing interests
The authors declare no competing interests.

Received: 1 November 2025 / Accepted: 26 February 2026
Published online: 03 March 2026

References

1. Khambete P, Harlow E, Ina J, Miskovsky S. Biomechanics of the Distal Tibiofibular Syndesmosis: A Systematic Review of Cadaveric Studies. Foot Ankle Orthop. 2021;6(2):24730114211012701.
2. Yao X, Wang C, Pan W, Chao Y, Tang J. Ankle syndesmotic ligaments avulsion fractures: incidence in adult population. J Orthop Surg Res. 2024;19(1):642.
3. Lin CF, Gross ML, Weinhold P. Ankle syndesmosis injuries: anatomy, biomechanics, mechanism of injury, and clinical guidelines for diagnosis and intervention. J Orthop Sports Phys Ther. 2006;36(6):372–84.
4. Mak MF, Gartner L, Pearce CJ. Management of syndesmosis injuries in the elite athlete. Foot Ankle Clin. 2013;18(2):195–214.
5. Wright RW, Barile RJ, Surprenant DA, Matava MJ. Ankle syndesmosis sprains in national hockey league players. Am J Sports Med. 2004;32(8):1941–45.
6. Vohra R, Singh A, Thorat B, Patel D. Instability of the distal tibiofibular syndesmosis. J Orthop Surg (Hong Kong). 2023;31(2):10225536231182349.
7. Sagi HC, Shah AR, Sanders RW. The functional consequence of syndesmotic joint malreduction at a minimum 2-year follow-up. J Orthop Trauma. 2012;26(7):439–43.
8. de-Las-Heras Romero J, Alvarez AML, Sanchez FM, et al. Management of syndesmotic injuries of the ankle. EFORT Open Rev. 2017;2(9):403–9.
9. Weening B, Bhandari M. Predictors of functional outcome following transsyndesmotic screw fixation of ankle fractures. J Orthop Trauma. 2005;19(2):102–8.
10. Kocadal O, Yucel M, Pepe M, Aksahin E, Aktekin CN. Evaluation of Reduction Accuracy of Suture-Button and Screw Fixation Techniques for Syndesmotic Injuries. Foot Ankle Int. 2016;37(12):1317–25.
11. Schepers T, Van Lieshout EM, Van der Linden HJ, De Jong VM, Goslings JC. Aftercare following syndesmotic screw placement: a systematic review. J Foot Ankle Surg. 2013;52(4):491–4.
12. van den Bekerom MP, Kloen P, Luitse JS, Raaymakers EL. Complications of distal tibiofibular syndesmotic screw stabilization: analysis of 236 patients. J Foot Ankle Surg. 2013;52(4):456–9.
13. Zhang P, Liang Y, He J, Fang Y, Chen P, Wang J. A systematic review of suture-button versus syndesmotic screw in the treatment of distal tibiofibular syndesmosis injury. BMC Musculoskelet Disord. 2017;18(1):286.
14. Kortekangas T, Savola O, Flinkkilä T, et al. A prospective randomised study comparing TightRope and syndesmotic screw fixation for accuracy and maintenance of syndesmotic reduction assessed with bilateral computed tomography. Injury. 2015;46(6):1119–26.
15. Laflamme M, Belzile EL, Bédard L, van den Bekerom MP, Glazebrook M, Pelet S. A prospective randomized multicenter trial comparing clinical outcomes of patients treated surgically with a static or dynamic implant for acute ankle syndesmosis rupture. J Orthop Trauma. 2015;29(5):216–23.
16. Xu G, Chen W, Zhang Q, Wang J, Su Y, Zhang Y. Flexible fixation of syndesmotic diastasis using the assembled bolt-tightrope system. Scand J Trauma Resusc Emerg Med. 2013;21:71.
17. Stenquist DS, Ye MY, Kwon JY. Acute and Chronic Syndesmotic Instability: Role of Surgical Stabilization. Clin Sports Med. 2020;39(4):745–71.
18. Kara AN, Esenyel CZ, Sener BT, Merih E. A different approach to the treatment of the lateral malleolar fractures with syndesmosis injury: the ANK nail. J Foot Ankle Surg. 1999;38(6):394–402.
19. Kabukcuoglu Y, Kucukkaya M, Eren T, Gorgec M, Kuzgun U. The ANK device: a new approach in the treatment of the fractures of the lateral malleolus associated with the rupture of the syndesmosis. Foot Ankle Int. 2000;21(9):753–8.
20. Wenny R, Duscher D, Meytap E, Weninger P, Hirtler L. Dimensions and attachments of the ankle ligaments: evaluation for ligament reconstruction. Anat Sci Int. 2015;90(3):161–71.
21. Clanton TO, Campbell KJ, Wilson KJ, et al. Qualitative and Quantitative Anatomic Investigation of the Lateral Ankle Ligaments for Surgical Reconstruction Procedures. J Bone Joint Surg Am. 2014;96(12):e98.
22. Golanó P, Vega J, de Leeuw PA, et al. Anatomy of the ankle ligaments: a pictorial essay. Knee Surg Sports Traumatol Arthrosc. 2016;24(4):944–56.
23. Williams BT, Ahrberg AB, Goldsmith MT, et al. Ankle syndesmosis: a qualitative and quantitative anatomic analysis. Am J Sports Med. 2015;43(1):88–97.
24. Campbell KJ, Michalski MP, Wilson KJ, et al. The ligament anatomy of the deltoid complex of the ankle: a qualitative and quantitative anatomical study. J Bone Joint Surg Am. 2014;96(8):e62.
25. Mondal S, Ghosh R. Experimental and finite element investigation of total ankle replacement: A review of literature and recommendations. J Orthop. 2019;18:41–9.
26. Pfaeffle HJ, Tomaino MM, Grewal R, et al. Tensile properties of the interosseous membrane of the human forearm. J Orthop Res. 1996;14(5):842–5.
27. Beumer A, van Hemert WL, Swierstra BA, Jasper LE, Belkoff SM. A biomechanical evaluation of the tibiofibular and tibiotalar ligaments of the ankle. Foot Ankle Int. 2003;24(5):426–9.
28. Liacouras PC, Wayne JS. Computational modeling to predict mechanical function of joints: application to the lower leg with simulation of two cadaver studies. J Biomech Eng. 2007;129(6):811–7.
29. Corazza F, O'Connor JJ, Leardini A, Parenti Castelli V. Ligament fibre recruitment and forces for the anterior drawer test at the human ankle joint. J Biomech. 2003;36(3):363–72.
30. van den Bekerom MP, Raven EE. The distal fascicle of the anterior inferior tibiofibular ligament as a cause of tibiotalar impingement syndrome: a current concepts review. Knee Surg Sports Traumatol Arthrosc. 2007;15(4):465–71.
31. Walke W, Paszenda Z, Kaczmarek M. Biomechanical analysis of tibia double threaded screw fixation. Arch Mater Sci Eng 2008;30(1): 41–4.
32. Gray HA, Taddei F, Zavatsky AB, Cristofolini L, Gill HS. Experimental validation of a finite element model of a human cadaveric tibia. J Biomech Eng. 2008;130(3):031016.
33. Sumanont S, Nopamassiri S, Boonrod A, Apiwatanakul P, Boonrod A, Phornphutkul C. Acromioclavicular joint dislocation: a Dog Bone button fixation alone versus Dog Bone button fixation augmented with acromioclavicular repair-a finite element analysis study. Eur J Orthop Surg Traumatol. 2018;28(6):1095–101.
34. Erkmen E, Simşek B, Yücel E, Kurt A. Three-dimensional finite element analysis used to compare methods of fixation after sagittal split ramus osteotomy: setback surgery-posterior loading. Br J Oral Maxillofac Surg. 2005;43(2):97–104.
35. Sikka RS, Fetzer GB, Sugarman E, et al. Correlating MRI findings with disability in syndesmotic sprains of NFL players. Foot Ankle Int. 2012;33(5):371–8.
36. Alastuey-López D, Seral B, Pérez MÁ. Biomechanical evaluation of syndesmotic fixation techniques via finite element analysis: Screw vs. suture button. Comput Methods Programs Biomed. 2021;208:106272.
37. Mercan N, Yıldırım A, Dere Y. Biomechanical Analysis of Tibiofibular Syndesmosis Injury Fixation Methods: A Finite Element Analysis. J Foot Ankle Surg. 2023;62(1):107–14.
38. Ebramzadeh E, Knutsen AR, Sangiorgio SN, Brambila M, Harris TG. Biomechanical comparison of syndesmotic injury fixation methods using a cadaveric model. Foot Ankle Int. 2013;34(12):1710–7.
39. Hu WK, Chen DW, Li B, Yang YF, Yu GR. Motion of the distal tibiofibular syndesmosis under different loading patterns: A biomechanical study. J Orthop Surg (Hong Kong). 2019;27(2):2309499019842879.
40. Burssens A, Krähenbühl N, Weinberg MM, Lenz AL, Saltzman CL, Barg A. Comparison of External Torque to Axial Loading in Detecting 3-Dimensional Displacement of Syndesmotic Ankle Injuries. Foot Ankle Int. 2020;41(10):1256–68.
41. Park S, Lee S, Yoon J, Chae SW. Finite element analysis of knee and ankle joint during gait based on motion analysis. Med Eng Phys. 2019;63:33–41.
42. Fraysse F, Arnold J, Thewlis D. A method for concise reporting of joint reaction forces orientation during gait. J Biomech. 2016;49(14):3538–42.
43. Kelly M, Vasconcellos D, Osman WS, et al. Alterations in tibiotalar joint reaction force following syndesmotic injury are restored with static syndesmotic fixation. Clin Biomech (Bristol). 2019;69:156–63.

44. Van Heest TJ, Lafferty PM. Injuries to the ankle syndesmosis. J Bone Joint Surg Am. 2014;96(7):603–13.
45. Jones CB, Gilde A, Sietsema DL. Treatment of Syndesmotic Injuries of the Ankle: A Critical Analysis Review. JBJS Rev. 2015;3(10):e1.
46. Schepers T, van Zuuren WJ, van den Bekerom MP, Vogels LM, van Lieshout EM. The management of acute distal tibio-fibular syndesmotic injuries: results of a nationwide survey. Injury. 2012;43(10):1718–23.
47. Bava E, Charlton T, Thordarson D. Ankle fracture syndesmosis fixation and management: the current practice of orthopedic surgeons. Am J Orthop (Belle Mead NJ). 2010;39(5):242–6.
48. Teramoto A, Suzuki D, Kamiya T, Chikenji T, Watanabe K, Yamashita T. Comparison of different fixation methods of the suture-button implant for tibiofibular syndesmosis injuries. Am J Sports Med. 2011;39(10):2226–32.
49. Parker AS, Beason DP, Slowik JS, Sabatini JB, Waldrop NE 3. rd. Biomechanical Comparison of 3 Syndesmosis Repair Techniques With Suture Button Implants. Orthop J Sports Med. 2018;6(10):2325967118804204.
50. Milstrey A, Lim WY, Wenda K, et al. Flexible syndesmotic reconstruction with two suture buttons provides equal stability compared to syndesmotic screws: a biomechanical study. Bioengineering. 2025;12(7):685.
51. Güvercin Y, Abdioğlu AA, Dizdar A, Yaylacı EU, Yaylacı M. Suture button fixation method used in the treatment of syndesmosis injury: A biomechanical analysis of the effect of the placement of the button on the distal tibiofibular joint in the mid-stance phase with finite elements method. Injury. 2022;53(7):2437–45.
52. Kikuchi S, Tajima G, Sugawara A, et al. Characteristic features of the insertions of the distal tibiofibular ligaments on three-dimensional computed tomography- cadaveric study. J Exp Orthop. 2020;7(1):3.
53. Jayatilaka MLT, Philpott MDG, Fisher A, Fisher L, Molloy A, Mason L. Anatomy of the Insertion of the Posterior Inferior Tibiofibular Ligament and the Posterior Malleolar Fracture. Foot Ankle Int. 2019;40(11):1319–24.
54. Fisher A, Bond A, Philpott MDG, et al. The anatomy of the anterior inferior tibiofibular ligament and its relationship with the Wagstaffe fracture. Foot Ankle Surg. 2021;27(3):291–5.
55. Haraguchi N, Armiger RS, Myerson MS, Campbell JT, Chao EY. Prediction of three-dimensional contact stress and ligament tension in the ankle during stance determined from computational modeling. Foot Ankle Int. 2009;30(2):177–85.
56. Jang CY, Kang KT, Hong H, et al. Mechanical stability of the proximal tibia with different bone formations after plate removal in medial opening-wedge high tibial osteotomy: a finite element analysis. J Orthop Surg Res. 2024;19(1):850.
57. Nault ML, Hébert-Davies J, Laflamme GY, Leduc S. CT scan assessment of the syndesmosis: a new reproducible method. J Orthop Trauma. 2013;27(11):638–41.
58. Liu Q, Zhao G, Yu B, Ma J, Li Z, Zhang K. Effects of inferior tibiofibular syndesmosis injury and screw stabilization on motion of the ankle: a finite element study. Knee Surg Sports Traumatol Arthrosc. 2016;24(4):1228–35.
59. McBryde A, Chiasson B, Wilhelm A, Donovan F, Ray T, Bacilla P. Syndesmotic screw placement: a biomechanical analysis. Foot Ankle Int. 1997;18(5):262–6.
60. Del Buono A, Florio A, Boccanera MS, Maffulli N. Syndesmosis injuries of the ankle. Curr Rev Musculoskelet Med. 2013;6(4):313–9.
61. Jordan TH, Talarico RH, Schuberth JM. The radiographic fate of the syndesmosis after trans-syndesmotic screw removal in displaced ankle fractures. J Foot Ankle Surg. 2011;50(4):407–12.
62. Wikerøy AK, Høiness PR, Andreassen GS, Hellund JC, Madsen JE. No difference in functional and radiographic results 8.4 years after quadricortical compared with tricortical syndesmosis fixation in ankle fractures. J Orthop Trauma. 2010;24(1):17–23.
63. Wójtowicz BG, Chawrylak K, Lesman J, et al. Routine Removal of Syndesmotic Screws After Tibiofibular Syndesmosis Fixation Does Not Affect Patient Function and Is Associated with a Higher Risk of Postoperative Complications. J Clin Med. 2025;14(10):3276.
64. Sanda II, Hosin S, Vermesan D, et al. Impact of Syndesmotic Screw Removal on Quality of Life, Mobility, and Daily Living Activities in Patients Post Distal Tibiofibular Diastasis Repair. Med (Kaunas). 2023;59(12):2048.
65. Bell DP, Wong MK. Syndesmotic screw fixation in Weber C ankle injuries–should the screw be removed before weight bearing? Injury. 2006;37(9):891–8.
66. Desouky O, Elseby A, Ghalab AH. Removal of Syndesmotic Screw After Fixation in Ankle Fractures: A Systematic Review. Cureus. 2021;13(6):e15435.
67. Meekaew P, Paholpak P, Wisanuyotin T, et al. Biomechanics comparison between endobutton fixation and syndesmotic screw fixation for syndesmotic injury ankle fracture; a finite element analysis and cadaveric validation study. J Orthop. 2022;34:207–14.
68. Klitzman R, Zhao H, Zhang LQ, Strohmeyer G, Vora A. Suture-button versus screw fixation of the syndesmosis: a biomechanical analysis. Foot Ankle Int. 2010;31(1):69–75.
69. Lee JS, Curnutte B, Pan K, Liu J, Ebraheim NA. Biomechanical comparison of suture-button, bioabsorbable screw, and metal screw for ankle syndesmotic repair: A meta-analysis. Foot Ankle Surg. 2021;27(2):117–22.
70. Tucker S, Milne I, Pitcher M, et al. A Review of Syndesmosis Injuries and Preferred Treatment in Football Players. Curr Rev Musculoskelet Med. 2025;18(5):190–200.
71. Grassi A, Samuelsson K, D'Hooghe P, et al. Dynamic Stabilization of Syndesmosis Injuries Reduces Complications and Reoperations as Compared With Screw Fixation: A Meta-analysis of Randomized Controlled Trials. Am J Sports Med. 2020;48(4):1000–13.
72. Marasco D, Russo J, Izzo A, et al. Static versus dynamic fixation of distal tibiofibular syndesmosis: a systematic review of overlapping meta-analyses. Knee Surg Sports Traumatol Arthrosc. 2021;29(11):3534–42.
73. Marqueen T, Owen J, Nicandri G, Wayne J, Carr J. Comparison of the syndesmotic staple to the transsyndesmotic screw: a biomechanical study. Foot Ankle Int. 2005;26(3):224–30.
74. ElRayes M, Hammoda A. Screw versus staple in stabilization of diastasis of tibiofibular syndesmosis. Foot Ankle Surg. 2007;13(1):5–9.
75. Thomas S, Berger G, O'Leary B, Brumm Z, Schwartz AK, Kent WT. Comparison of tibiofibular syndesmosis stability following treatment of proximal, middle, and distal third fibula fractures. Eur J Orthop Surg Traumatol. 2025;35(1):53.
76. Kuhn AW, Coughlin MJ, McGonegle SJ, et al. Distal Tibiofibular Syndesmosis Injuries in the National Football League (NFL): A Spectrum of Pathology That Correlates With Time to Return to Full Participation. Sports Health. 2025;17(2):404–11.
77. Dahmen J, Jaddi S, Hagemeijer NC, et al. Incidence of (Osteo)Chondral Lesions of the Ankle in Isolated Syndesmotic Injuries: A Systematic Review and Meta-Analysis. Cartilage. 2022;13(2):19476035221102569.
78. Walinga AB, Dahmen J, Stornebrink T, Emanuel KS, Kerkhoffs GMMJ. Fifteen out of 16 elite athletes showed concomitant low-grade cartilage lesions of the ankle with unstable syndesmotic injuries: concerns from a prospective case series. BMJ Open Sport Exerc Med. 2024;10(1):e001879.
79. Mercan N, Yurteri A, Dere Y. Do lateral ankle ligaments contribute to syndesmotic stability: a finite element analysis study. Comput Methods Biomech Biomed Engin. 2024;27(13):1768–80.
80. Weiss JA, Maker BN, Govindjee S. Finite element implementation of incompressible, transversely isotropic hyperelasticity. Comput Methods Appl Mech Eng. 1996;135(1–2):107–28.
81. Pierrat B, Murphy JG, MacManus DB, Gilchrist MD. Finite element implementation of a new model of slight compressibility for transversely isotropic materials. Comput Methods Biomech Biomed Engin. 2016;19(7):745–58.

Publisher's Note